Changes in physical properties of rocks during serpentinization and implications for natural hydrogen exploration

Yashee Mathur
Department of Energy Science and Engineering
Stanford University
yashee@stanford.edu

Tapan Mukerji
Department of Energy Science and Engineering
Stanford University
mukerji@stanford.edu

Version: Jan 16th, 2024

This is a non-peer-reviewed preprint submitted to EarthArXiv. This paper is under review and is submitted to the *The Leading Edge* special issue honoring Amos Nur

Changes in physical properties of rocks during serpentinization and implications for natural hydrogen exploration

Yashee Mathur[1], Tapan Mukerji[1,2,3]
[1]*Department of Energy Science & Engineering, Stanford University*
[2]*Department of Geophysics, Stanford University*
[3]*Department of Earth & Planetary Sciences, Stanford University*

Abstract

Serpentinization, transforms the physical properties of ultramafic rocks, with significant implications for natural hydrogen exploration. This study compiles and analyzes over 1,000 samples from diverse geological settings to elucidate relationships between rock properties—such as density, seismic velocities, elastic moduli, porosity, and magnetic susceptibility—and the degree of serpentinization. Our findings reveal systematic trends, including marked reductions in density and seismic velocities, and increases in porosity and magnetic susceptibility, which can serve as measurable proxies for identifying hydrogen-rich source rocks. By establishing robust empirical and cross-property relationships, we offer predictive rock physics tools to enhance geophysical exploration and reduce interpretation uncertainties in hydrogen exploration. Furthermore, this work uses differential effective medium models to capture rock property changes during serpentinization, laying the groundwork for further rock physics modeling. These insights not only improve the understanding of subsurface hydrogen systems but also pave the way for innovative exploration strategies in the growing field of natural hydrogen exploration.

1. Introduction

Rock physics plays a tremendous role in quantitative seismic interpretation for oil and gas resources by providing the critical link between petrophysical rock and fluid properties and their associated elastic and seismic signatures. Many rock physics relations and models have been established for oil and gas resources, pioneered by the work of Amos Nur and others. Natural hydrogen is a carbon-free, new source of clean energy for the future. Despite the potential game-changing impact on clean energy and the environment, natural H_2 exploration is still in the early stages. What are the possible geophysical signatures of geological hydrogen occurrence? What are some of the rock physics relations and models that can be used to explore for natural hydrogen?

Serpentinization of iron-rich rocks is one of the notable reactions responsible for generating natural hydrogen (Truche, McCollom, and Martinez 2020; Coveney Jr. et al. 1987) amongst others (Boreham et al. 2021; Klein, Tarnas, and Bach 2020). Although there is extensive literature available for changes in *geochemical* composition during serpentinization and controls on hydrogen generations, there exists very limited literature on the associated *rock physics* relations (Frery et al. 2021; Nicolas Lefeuvre et al. 2021; Fuad et al. 2023; Li et al. 2020a; N. Lefeuvre et al. 2022). The extent of hydrogen production during serpentinization is governed by factors such as the composition of protolith, thermodynamic conditions, temperature, pressure, salinity, pH, water-rock ratio and presence of specific trace metals (McCollom et al. 2020; 2016; Klein, Bach, and McCollom 2013; H. M. Miller et al. 2017; Lamadrid et al. 2017; Huang et al. 2019; Leong et al. 2023; Andreani, Daniel, and Pollet-Villard 2013). Along with natural serpentinization reactions, iron-rich rocks can also be geo-engineered to produce hydrogen termed as stimulated hydrogen (Osselin et al. 2022; Templeton et al. 2024). During serpentinization, the formation of new mineral

assemblages causes the rheology and the physical properties of rocks such as density, magnetic susceptibility, and seismic velocity, to change (D. J. Miller and Christensen 1997; Oufi 2002; Toft, Arkani-Hamed, and Haggerty 1990; Klein and Le Roux 2020; Stesky and Brace 1973; Yoshino, Manthilake, and Pommier 2024). Although the interest in serpentinization and ultramafic rocks from a natural hydrogen standpoint is recent, the data related to these changes has been present and studied over decades. Since serpentinization is one of the major reactions in mantellic rocks, the associated changes in physical properties have been studied extensively to understand the mantle's composition, and plate tectonics (Birch 1969; Hatakeyama and Katayama 2020; Keppler, Ohtani, and Yang 2024; Durand, Juriček, and Fischer 2024). The current study compiles more than 1000 samples from the literature from different geological environments (Li et al. 2020b; Hatakeyama and Katayama 2020; Falcon-Suarez et al. 2017; Watanabe, Kasami, and Ohshima 2007; Oufi 2002; D. J. Miller and Christensen 1997; Kroenke et al. 2013; Horen, Zamora, and Dubuisson 1996; Cutts et al. 2021; Kern and Tubia 1993; Toft, Arkani-Hamed, and Haggerty 1990; Christensen 1978; D. J. Miller, Iturrino, and Christensen 1996; Christensen and Salisbury 1972; Christensen 1966; Bonnemains et al. 2016) to understand the change in rock properties during serpentinization. We analyze the effect of serpentinization on density, magnetic susceptibility, velocities, and elastic properties and provide rock physics regression relationships between the degree of serpentinization and physical properties.

2. Material and methods

Data were collected from the literature as shown in **Table 1.** They come from different locations and geological settings, spanning various lithologies including variably serpentinized peridotite and pyroxenites. In our compilation, we chose lower pressure range measurements (~ 20-50 MPa or lower) appropriate for depths suitable for natural hydrogen exploration.

Table 1: Location, geological setting, rock types, distribution of physical properties, and number of samples for all the compiled data. ρ-density, k- magnetic susceptibility, V_P- Compressional wave velocity, V_S-Shear wave velocity, ϕ= porosity.

Location	Geological Setting	Dominant lithology	Physical Properties	No. of samples	Reference
Western Canadian Cordillera	Ophiolitic massifs	Ultramafic rocks	ρ, k	418	(Cutts et al. 2021)
Zedang Ophiolite, Tibet	Ophiolites	Lherzolite, harzburgite	ρ, k	21	(Li et al. 2020a)
Mineoka belt, Japan and South Mariana and Tonga trenches	Accretionary prism and deep-sea floor	Lizardite, chrysotile	ρ, ϕ, V_P, V_S	4	(Hatakeyama and Katayama 2020)
Atlantis Massif, Mid-Atlantic Ridge (MAR)	Ophiolite complexes	Serpentinized peridotite	ρ, ϕ	4	(Falcon-Suarez et al. 2017)
Papua New Guinea	Ophiolitic rocks	Harzburgite, pyroxenite	V_P, V_S, ρ	12	(Kroenke et al. 2013)
Hida outer belt, Central Japan	Mantle wedge	Partially serpentinized peridotite	V_P, V_S, ρ		(Watanabe, Kasami, and Ohshima 2007)

Pindos, Oman, France	Ophiolite complex	Variably serpentinized peridotites	ρ, ϕ, k	44	(Bonnemains et al. 2016)
MAR and Hess Deep	Oceanic crust	Serpentinized abyssal peridotites	ρ, k	245	(Oufi 2002)
MAR, South of Kane Transform Zone (MARK)	Mid-oceanic ridge	Serpentinized harzburgite, pyroxene-rich serpentinized harzburgite, metagabbro, gabbro, olivine gabbro, troctolite	V_P, V_S, ρ	66	(D. J. Miller and Christensen 1997)
Xigaze ophiolite (Tibet)	Ophiolite complex	Serpentinized harzburgite	ρ, ϕ, V_P, V_S	6	(Horen, Zamora, and Dubuisson 1996)
Ronda peridotites, Southern Spain	Ophiolitic massifs	Dunite, harzburgite, lherzolite	V_P, V_S, ρ	14	(Kern and Tubia 1993)
Josephine peridotite (Oregon)	Ophiolites	Serpentinized harzburgites	ρ, k	39	(Toft, Arkani-Hamed, and Haggerty 1990)
Western United States	Ophiolites	Serpentinites, metagabbro, diabase, gabbro, pyroxenite	V_P, V_S, ρ	35	(Christensen 1978)
Mid-Atlantic Ridge	Oceanic crust	Serpentinites	V_P, V_S, ρ	3	(Christensen 1972)
Different locations across California, Washington and Oregon	Ophiolites	Peridotite, dunite partially serpentinized peridotite and dunite, serpentinite	V_P, V_S, ρ	11	(Christensen 1966)

3. Serpentinization induced changes in rock properties

An increase in volume and a decrease in density are inevitable in isochemical serpentinization (Toft, Arkani-Hamed, and Haggerty 1990). Broadly, during serpentinization, the density, velocity, and different elastic moduli decrease, while magnetic susceptibility and Poisson's ratio increase. In some cases, substantial volume increase of up to 40% occurs during serpentinization that can be accommodated by fracturing, thus further exposing fresh rock surfaces (Klein and Le Roux 2020). In this section, we will explore the relationships of different physical properties with serpentinization along with relevant cross property relationships.

3.1. Elastic and Seismic Properties

3.1.1. Density, Velocity (V_P, V_S) and Acoustic impedance vs Serpentinization

The most studied and pervasive change during serpentinization is the marked reduction in density **(Figure 1)**. The average density of pristine peridotites, ~ 3.1-3.3gm/cm^3, is much higher than that of pure serpentinite ~ 2.55-2.6 gm/cm^3 (Mével 2003). Thus, change in density has also been used to calculate the extent of serpentinization when direct measurements of the mineral constituents are not available. **Figure 1** shows a least squares regression fitted to the data with an R^2 value of 0.888. Popular regression relationships given by (D. J. Miller and Christensen 1997; Cutts et al. 2021) are also plotted. The *Miller and Christensen'97* line overlaps our line at higher densities whereas *Cutts et al., '21* line overlaps with our fit at lower densities. A few samples show densities lower than pure serpentinites. This might be a porosity effect. For instance, the lowest density sample is from the Tonga trench region (Hatakeyama and Katayama 2020) and has a porosity of 25.8%.

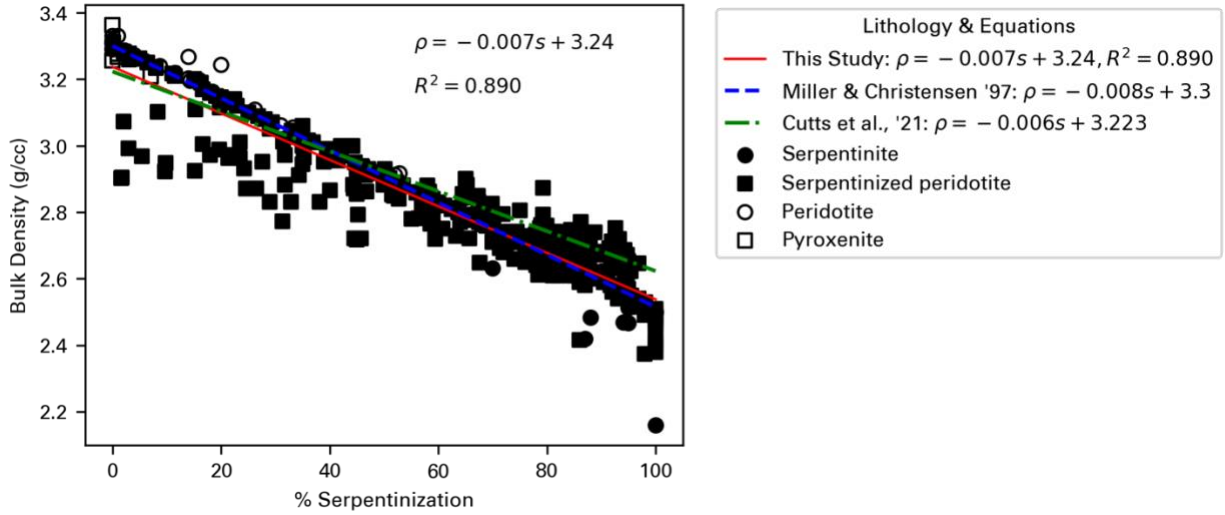

Figure 1: Bulk density vs serpentinization % (s) with fitted regression relationships from the current study as well as from D. J. Miller and Christensen 1997; and Cutts et al. 2021.

Density monitoring using well logs and gravity or muon tomography measurements (Schouten, Furseth, and van Nieuwkoop 2022) has been carried out widely for resource exploration. Thus, the change in density can be quickly applicable to either image rocks that are undergoing natural serpentinization or monitor changes in density during stimulated hydrogen production to ascertain the extent of serpentinization.

Seismic properties of ultramafic rocks vary with their proportion of olivine to pyroxene and abundances of accessory minerals formed during serpentinization, (Christensen 2004). P-wave velocities for monomineralic aggregates of olivine, pyroxene, and serpentine approximate 8.54, 7.93, and 5.10 km/sec, respectively. Corresponding S-wave velocities are 4.78, 4.65, and 2.35 km/sec. (Christensen 1966). Along with density, both P and S wave velocities as well as acoustic impendence (P-wave impedance) decrease with serpentinization **(Figure 2 a, b,c)**. There is a ~40% decrease in P-wave velocity, ~60% decrease in S-wave velocity, and ~60% decrease in acoustic impendence with 100% serpentinization. This velocity decrease has been used to estimate the degree of serpentinization in the oceanic mantle for quite some time (Christensen 2004). One caution here is at low pressures and temperatures, velocity not only depends on serpentinization but also on fluid-filled porosity and preferred mineral orientation (Hatakeyama and Katayama

2020). The compiled data is fitted using least square regression with an R^2 value of 0.976, 0.937, and 0.973 for V_P, V_S, and acoustic impendence vs serpentinization respectively. We rejected two outlier peridotite samples which had very low velocity and were described to have very loose grains (Christensen 1966). Similarly, two very high velocity serpentinites were rejected as outliers as they contained antigorite, a high-temperature serpentinite not relevant to our study.

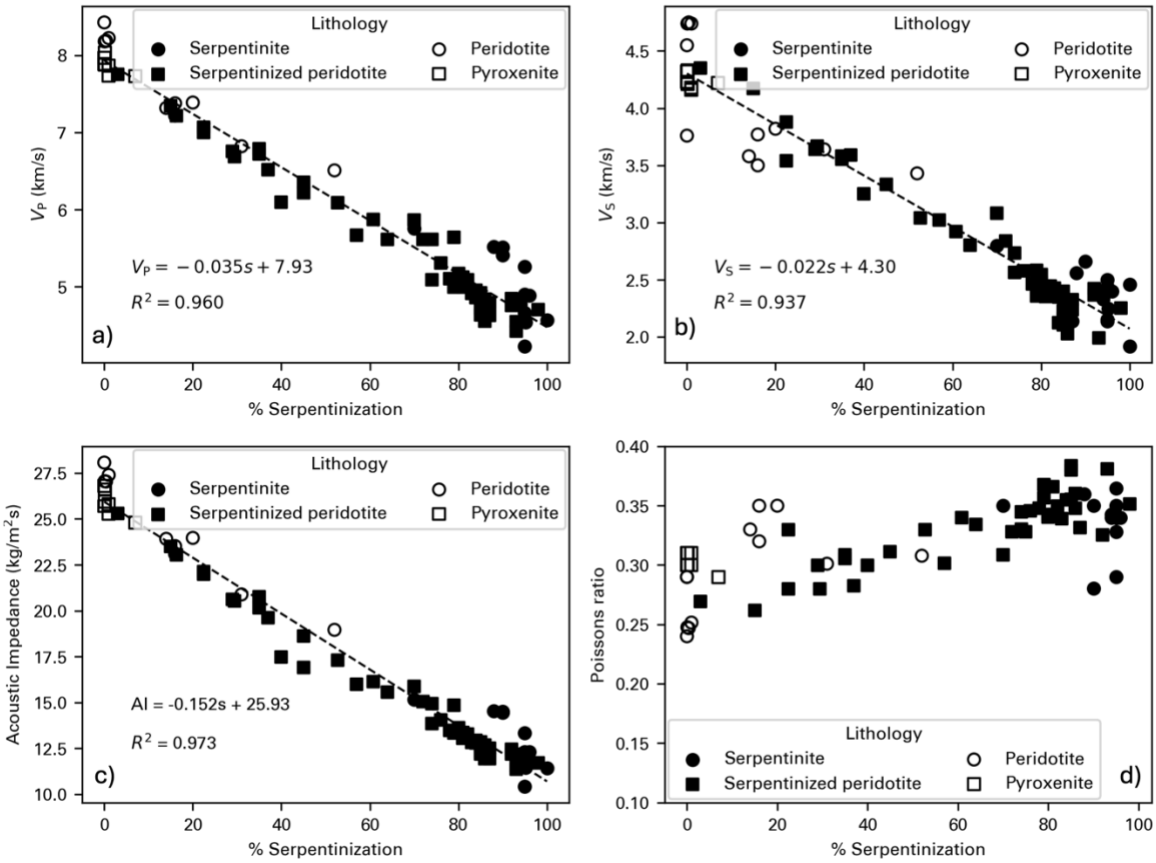

Figure 2: a) Compressional wave velocity (V_P), b) Shear wave velocity (V_S), c) Acoustic impedance d) Poisson's ratio vs serpentinization % (s) and fitted regression relationship.

Serpentinized peridotites have low velocities and high Poisson's ratio. Serpentinite has a distinctly high Poisson's ratio relative to most other silicate rocks, theoretically allowing it to be distinguished from other rocks in ophiolite complexes (D. J. Miller and Christensen 1997). **Figure 2d** shows the increase in Poisson's ratio with serpentinization from 0.25-0.3 for ultramafic rocks to 0.3-0.4 for highly serpentinized rocks. The presence of magnetite in highly serpentinized peridotites can also lower the Poisson's ratio.

3.1.2. V_P/V_S Ratio and Acoustic Impedance (AI)

The V_P/V_S ratio vs acoustic impendence plot is a standard rock physics template (RPT) (Chi and Han 2009; Odegaard and Avseth 2004; Avseth et al. 2010a) and has been used to distinguish between different lithologies as well as distinguish different fluids. **Figure 3** shows that the V_P/V_S ratio increases with serpentinization except for some samples with low V_P/V_S and acoustic

impendence possibly due to very high porosity. Samples that have been less than ~50% serpentinized show V_P/V_S of 2 and acoustic impedance > 17.5 Mkg/m^{2}s whereas samples with greater than 50% serpentinization are marked by high V_P/V_S of 2-2.3 and a lower acoustic impedance between 10-15 Mkg/m^{2}s. This provides a clear distinction between highly serpentinized samples that might have low potential to generate hydrogen vs samples that might yet produce hydrogen.

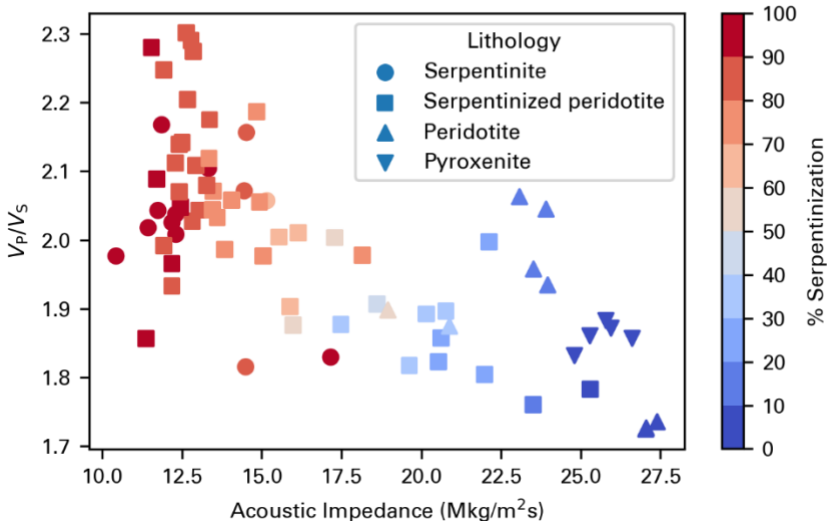

Figure 3: VP/VS vs acoustic impendence colored as per the degree of serpentinization.

3.1.3. V_P vs V_S

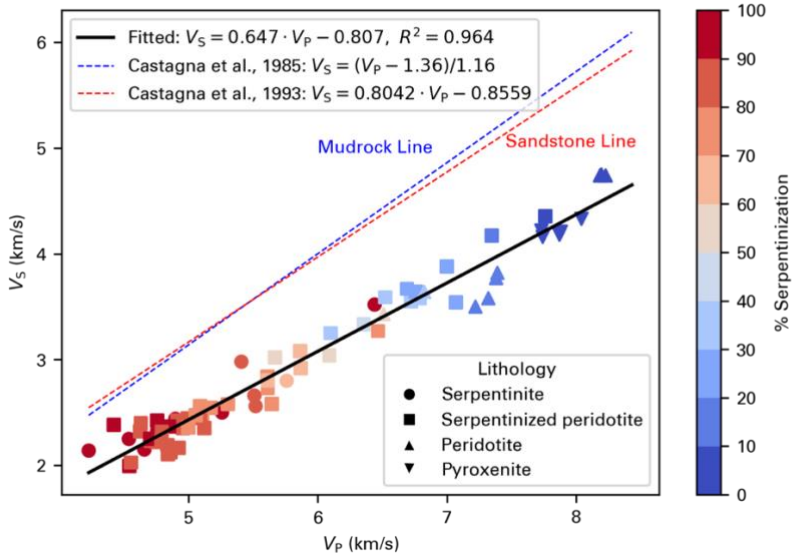

Figure 4: V_S vs V_P and their fitted regression along with popular regression lines for sandstone and mud rock given by (John P Castagna, Batzle, and Eastwood 1985; J P Castagna et al. 1993). *Points are colored by the degree of serpentinization.*

AVO analysis and V_P -V_S relations have been key to the determination of lithology and fluids in hydrocarbon exploration. As a result, there are a wide variety of published V_P-V_S relations for

hydrocarbon reservoirs and cap rocks. **Figure 4** cross plots V_S vs V_P for rocks relevant to natural hydrogen fitted with a linear regression with an R^2 of 0.964. Three outlier samples that showed high porosity > 5% were not included in the fitting and plot outside the linear fit. Popular sandstone (J P Castagna et al. 1993) and mudrock (John P Castagna, Batzle, and Eastwood 1985) lines are also shown in **Figure 4** highlighting the difference between ultramafic rocks and sedimentary rocks but also indicating that the same templates used in hydrocarbon exploration, after adaptation, can be used for hydrogen exploration.

3.1.4. Rock Elastic Moduli Changes

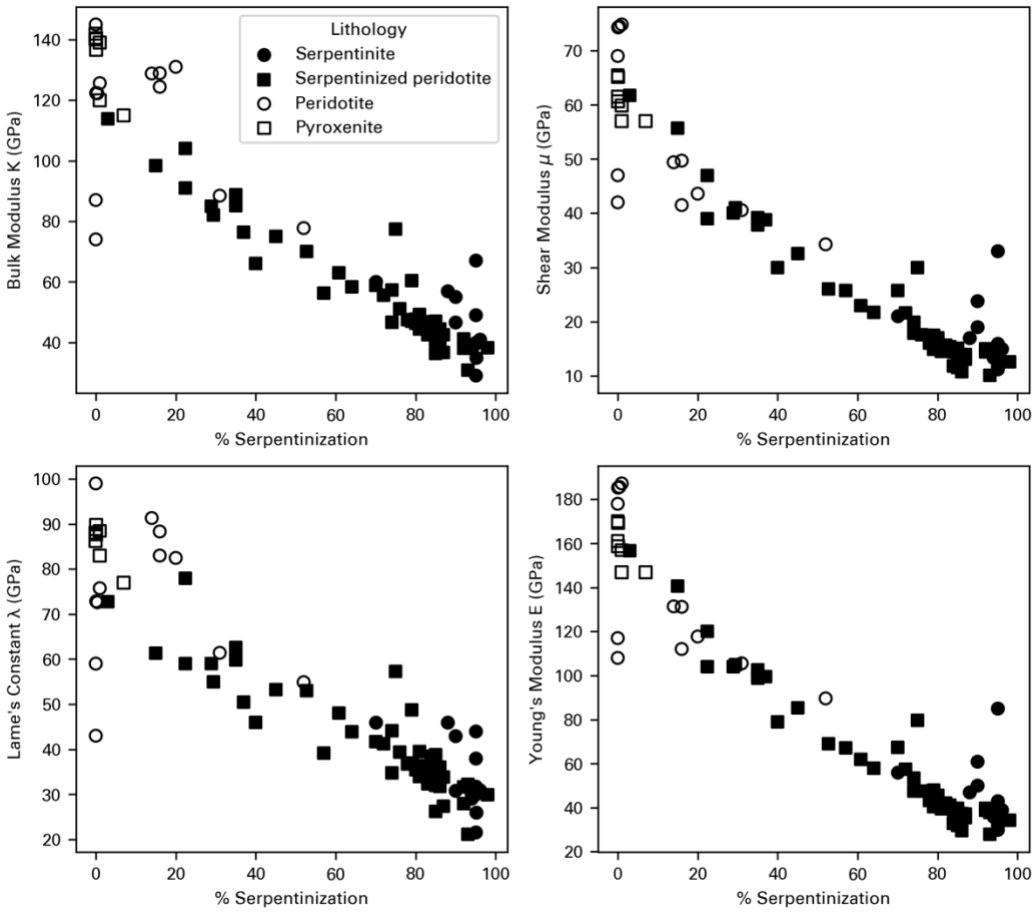

Figure 5: Change in different rock moduli with serpentinization; bulk modulus (top left), shear modulus (top right), Lame's constant (bottom left) and Young's modulus (bottom right)

Bulk modulus (K), shear modulus (μ), Lame's constant (λ), and Young's modulus (E) are fundamental parameters quantifying a rock's mechanical and elastic behavior under stress and have been used extensively to infer geomechanical properties, lithology, and fluid content. The different moduli show a decreasing trend with serpentinization as expected **(Figure 5)**.

Effective Medium Modeling

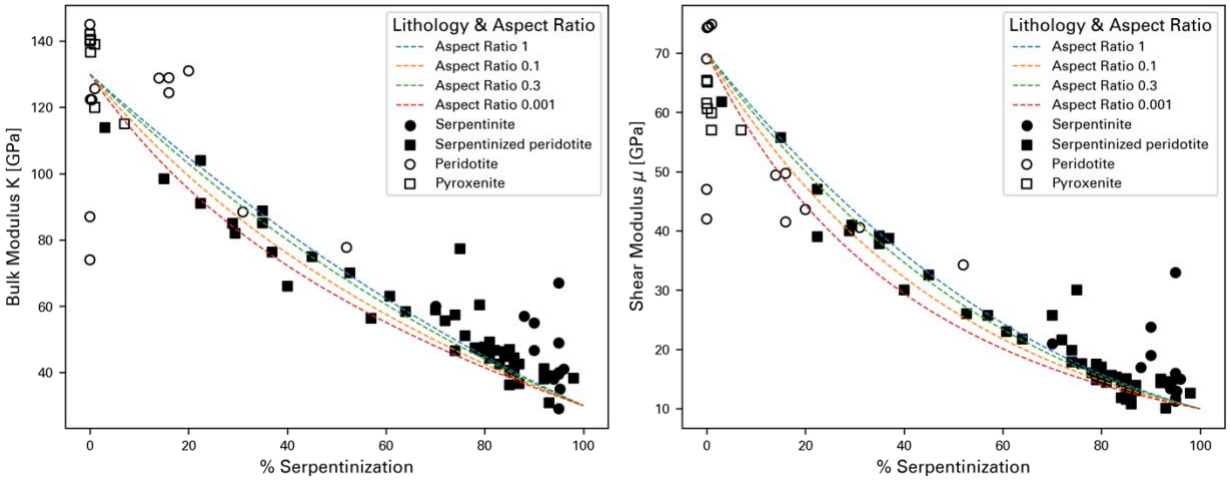

Figure 6: Bulk modulus(left) and shear modulus (right) vs serpentinization and effective rock moduli calculated using DEM inclusion model with varying aspect ratios (Zimmerman 1990; Norris 1985).

(R. L. Carlson 2001) fitted a Hashin-Strikman (HS) and Voigt-Reuss-Hill (VRH) average models to bulk and shear modulus data for partially serpentinized peridotites from (Christensen 1966; Christensen and Salisbury 1972; Christensen 1978). In this study, as shown in **Figure 6,** we fit a Differential Effective Medium (DEM) inclusion model (Zimmerman 1990; Norris 1985) with varying aspect ratios. The DEM model allows the addition of inclusions incrementally to the host material and tracks the effective properties of the combined medium progressively. The bulk and shear moduli of olivine and serpentinite taken for this modeling along with the aspect ratios are given in **Table 2.** The DEM model fits well the data acquired at different locations and from variably serpentinized peridotites.

Table 2: Moduli for peridotite and serpentine used for DEM modeling

Property	Olivine [Reference]	Serpentine
Bulk Modulus (GPa)	130 (Schön 2015)	30
Shear Modulus (GPa)	70	10
Aspect ratio		1, 0.3,0.1,0.001

In **Figure 7,** we model the simultaneous process of increasing serpentinization and hydrogen generation as serpentinization proceeds. The total volume fraction of inclusion added at each incremental step is partitioned into fractions of incrementally added serpentine and hydrogen. **Figure 7** (left) is the plot between the fraction of hydrogen generated vs the fraction of serpentinization and in **Figure 7** (right) we plot bulk modulus vs the % of olivine (i.e., the initial protolith). We assume two models for the fractionation between serpentine and hydrogen – a linear model and a quadratic model with the ratio of serpentine to the total inclusion volume given by equations 6 and 7 respectively. The fraction of serpentine and hydrogen inclusions are calculated by equations 8 and 9. For **Figure 7** r_0 is 0.7 and a, b, and c are 0.99, 0.3 and 0.1 respectively.

$$r_{serpentine} = r_0 \tag{2}$$

$$r_{serpentine} = \max\left(0, \min\left(1, a - b\phi_{inclusion} - c\,\phi_{inclusion}{}^2\right)\right) \tag{1}$$

$$\phi_{serpentine} = \phi_{inclusion} \cdot r_{serpentine} \quad (3)$$

$$\phi_{hydrogen} = \phi_{inclusion} \cdot (1 - r_{serpentine}) \quad (4)$$

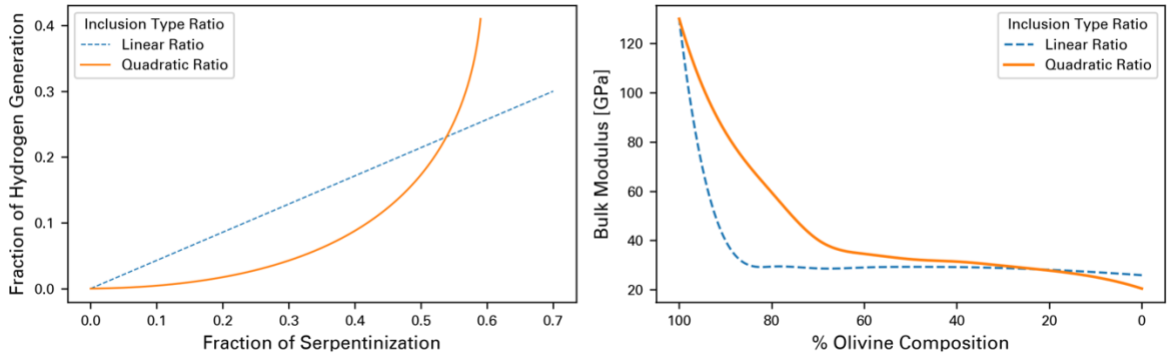

Figure 7: (left) Fraction of hydrogen vs fraction of serpentine in the total inclusions for linear and quadratic models, (right) bulk modulus vs % olivine composition as serpentinization proceeds with hydrogen generation for both linear and quadratic models.

3.2. Magnetic Susceptibility vs Serpentinization

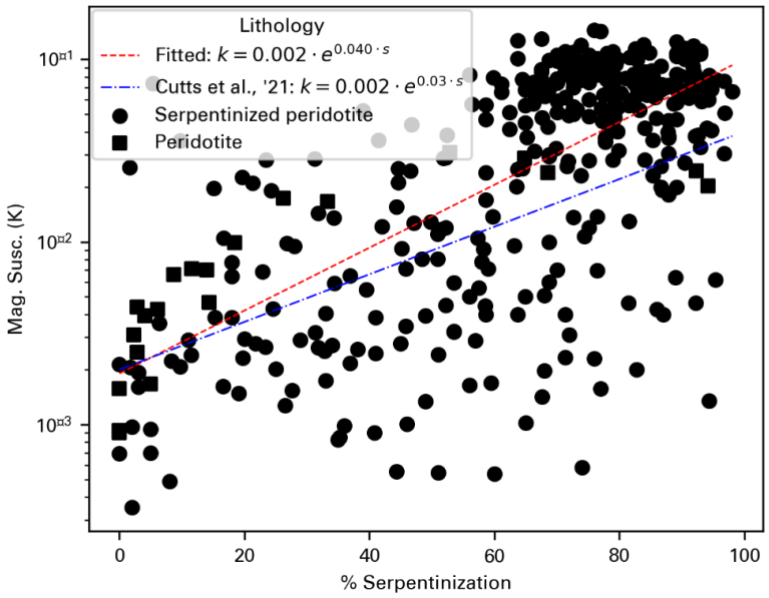

Figure 8: Magnetic Susceptibility (K) vs % Serpentinization(s) with regression relationship fitted from current study and (Cutts et al. 2021)

Figure 8 shows the variation of magnetic susceptibility with serpentinization, the *Cutt's et al. (2021)* relation and our fitted relationship with an R^2 of 0.12. Broadly, magnetic susceptibility increases with serpentinization, due to the formation of magnetite. In general, serpentinization of olivine leads to the formation of magnetite, while the serpentinization of orthopyroxene and orthopyroxene-rich rocks often occurs without producing magnetite. Notably, olivine serpentinization does not invariably result in magnetite formation. The initial stages of

serpentinization are marked by a relative scarcity of magnetite, followed by significant magnetite formation, accompanied by a characteristic decrease in fluid pH. The formation of magnetite also correlates to higher hydrogen generation. This can be measured, and hydrogen generation can be approximated using magnetic susceptibility (H. M. Miller et al. 2017). However, the data also suggests that based on the variable conditions of serpentinization, the formation and the quantity of magnetite varies. Thus, only using magnetic susceptibility as an indication of serpentinization is not recommended.

3.3. Cross-Property Relationships

3.3.1. Magnetic Susceptibility vs Density

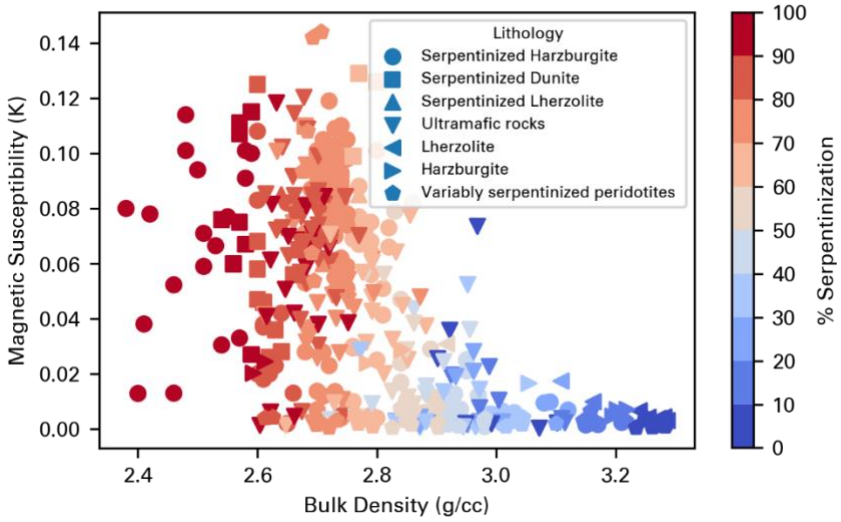

Figure 9: Magnetic susceptibility vs Bulk density colored as per % serpentinization

Figure 9 shows that as density decreases, magnetic susceptibility increases during serpentinization. Changes in density during serpentinization is primarily linked to a rock's mineralogy change whereas changes in magnetic susceptibility is related to the concentration and distribution of ferro-magnetic minerals such as magnetite. As per **Figure 9,** <50% serpentinized samples do not show a magnetic susceptibility > 20×10^{-3} (SI) inferring that magnetite might be formed in the later stages of serpentinization consistent with observations from (Li et al. 2020b; Cutts et al. 2021) and (Bach et al. 2006). (Cutts et al. 2021) argues that there are two magnetic susceptibility trends during serpentinization: one involves a 100-fold increase in magnetic susceptibility and is followed by most harzburgitic samples, whereas the second involves very little change in magnetic susceptibility and is followed by most dunitic samples. (Maffione et al. 2014) argues that above 60% the system moves from a rock dominated closed system to a fluid dominated open system resulting in an exponential increase in magnetite formation. This aligns well with **Figure 9,** where below 50-60% serpentinization, we observe a linear decrease in density and almost no increase in susceptibility. Above 60% serpentinization, the magnetic susceptibility increases exponentially. Broadly, although the decrease in density is predictable, the formation of magnetite and increase in magnetic susceptibility during serpentinization varies with a lot of different parameters namely protolith composition, temperature, water-rock ratio etc,. So, while an increase in magnetic susceptibility indicates the formation of hydrogen and serpentinization, the converse might not be true.

3.3.2. Density vs Velocity

Seismic P-wave velocity and density are positively correlated, and both decrease with serpentinization (**Figure 10).** The dataset is fitted using a power law and a linear model with R^2 > 0.9. These relationships can give a first-order approximation of density if seismic data are acquired for hydrogen exploration or to estimate velocity from gravity data. We also plot popular relationships for sandstones (Gardner, Gardner, and Gregory 1974), (Godfrey, Beaudoin, and Klemperer 1997).

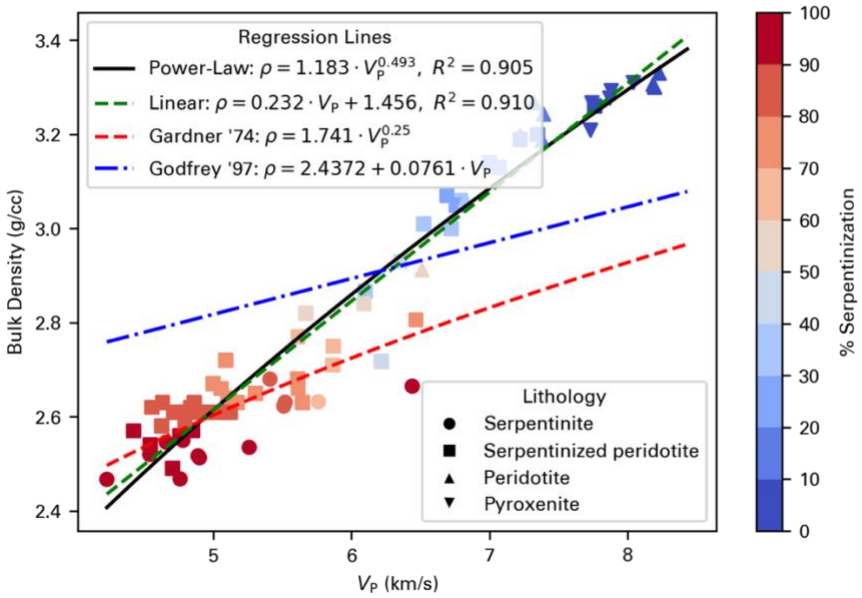

Figure 10: Bulk density vs P-velocity with fitted regression relation plotted along with popular relationships given by (Gardner, Gardner, and Gregory 1974; Godfrey, Beaudoin, and Klemperer 1997) *for other lithologies. Points are colored based on % serpentinization.*

4. Discussion

4.1. Implications for Geophysical Modeling and Interpretation

This study establishes rock physics relationships for different geophysical and rock properties during serpentinization that can affect natural hydrogen generation. The established rock physics relationships can aid multiphysics interpretation workflows including gravity, electromagnetic, electrical, and seismic data to explore geologic hydrogen better. The rock physics relationships can further provide constraints to field interpretations and reduce uncertainty. While electrical conductivity might be sensitive to the presence of hydrogen, we did not study it extensively here. Although a conductivity anomaly is non-unique, the presence of hydrogen has been argued to increase the electrical conductivity in tectonic settings such as subduction zones (Yoshino, Manthilake, and Pommier 2024). Another factor is changes in seismic anisotropy during serpentinization (Christensen 2004; Watanabe, Kasami, and Ohshima 2007). It is argued that the alignment of olivine crystal is weakened during serpentinization leading to the formation of relatively isotropic serpentine (Horen, Zamora, and Dubuisson 1996). The current dataset did not

show any such strong correlation. A more detailed study on seismic anisotropy and serpentinization should be conducted.

4.2. Interpretation pitfalls

Based on the composition of the protolith, a wide variety of serpentinization reaction pathways are possible (Toft, Arkani-Hamed, and Haggerty 1990). Ultramafic rocks can co-exist with fresh or altered mafic rocks such as gabbro, and metagabbro **(Figure 11).** Serpentinites and serpentinized harzburgites show low values for V_P and V_S but partially serpentinized peridotites are interspersed with mafic rocks like diabase, spilite, olivine gabbro and metagabbro **(Figure 11).** On the higher velocity end, peridotites are again separated from the rest of the rocks. This is consistent with the observations of (Mével 2003; Richard L Carlson and Miller 1997; Iturrino et al. 1991; Dewandel et al. 2003) who propose that P- and S-wave velocities and density of partially serpentinized rocks are in the same range as fresh or altered mafic rocks. Thus, only relying on a single physical property might not yield accurate predictions about serpentinization. However, integrating multiple properties within the geological context would reduce ambiguity.

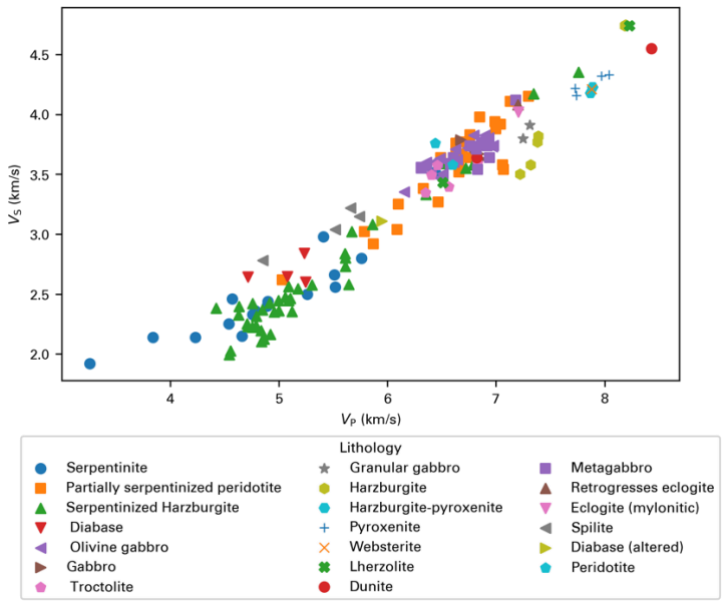

Figure 11: V_P vs V_S relationship of all the samples compiled colored as per their lithology.

5. Summary and conclusion

This study investigates the role of rock physics relations in the geophysical interpretation of geologic hydrogen resources, with a focus on serpentinization of ultramafic rocks as a natural mechanism for hydrogen generation. Serpentinization alters critical rock properties such as density, seismic velocities, porosity, and magnetic susceptibility, providing measurable indicators for identifying and characterizing hydrogen source rocks and reservoirs. By integrating and data mining over 1,000 rock sample measurements from the literature from diverse geological settings, this work establishes rock property relationships and models the geophysical responses to serpentinization These trends can be useful for natural hydrogen exploration and monitoring of

stimulated natural hydrogen. All the rock physics relations established in this study are collated in **Table 3.**

Table 3: Regression relationships between different physical properties and their respective R-squared values. The equations are at pressures < 50 MPa and low temperature.

Properties	Equation(s)	R^2
Density vs Serpentinization	$\rho = -0.007s + 3.24$	0.888
P-wave velocity vs Serpentinization	$V_P = -0.035s + 7.93$	0.96
S-wave velocity vs Serpentinization	$V_S = -0.022s + 4.3$	0.937
Acoustic Impedance vs Serpentinization	$AI = -0.152s + 25.93$	0.973
Mag. Susceptibility vs Serpentinization	$K = 0.002 \cdot e^{0.04s}$	
S-wave velocity vs P-wave velocity	$V_S = 0.647 \cdot V_P - 0.807$	0.964
S-wave velocity vs P-wave velocity and Serpentinization	$V_S = 0.585V_P - 0.002s - 0.308$	0.966
Density vs P-wave velocity	$\rho = 1.183 \cdot {V_P}^{0.493}$ $\rho = 0.232 \cdot V_P + 1.456$	0.905 0.91
Density vs P-wave velocity and Serpentinization	$\rho = 2.779\, {V_P}^{0.084} - 0.007s$ $\rho = 0.049\, V_P - 0.007s + 2.918$	0.977 0.978

Despite the advancements presented in this study, challenges remain. Variations in rock properties across different geological settings emphasize the need for localized calibration. Furthermore, the effects of fluid composition and pressure variations on geophysical responses require more detailed investigations. The development of joint inversion techniques and advanced multiphysics modeling will be essential for fully exploiting the complementary strengths of different geophysical methods. This work not only enhances the understanding of geophysical responses to serpentinization but also establishes a rock physics foundation for future research and technological innovation in natural hydrogen prospecting.

Acknowledgements
We acknowledge funding from the sponsors of the Stanford Natural Gas Initiative (NGI) and the Stanford Center for Earth Resources Forecasting (SCERF). We are indebted to Amos Nur for his pioneering foresight, vision, and leadership in laying the foundations for rock physics and its applications in the geoscience energy industry.

References

Andreani, Muriel, Isabelle Daniel, and Marion Pollet-Villard. 2013. "Aluminum Speeds up the Hydrothermal Alteration of Olivine." *American Mineralogist* 98 (10): 1738–44. https://doi.org/10.2138/am.2013.4469.

Avseth, Per, Tapan Mukerji, Gary Mavko, and Jack Dvorkin. 2010a. "Rock-Physics Diagnostics of Depositional Texture, Diagenetic Alterations, and Reservoir Heterogeneity in High-Porosity Siliciclastic Sediments and Rocks—A Review of Selected Models and Suggested Work Flows." *Geophysics* 75 (5): 75A31–47.

———. 2010b. "Rock-Physics Diagnostics of Depositional Texture, Diagenetic Alterations, and Reservoir Heterogeneity in High-Porosity Siliciclastic Sediments and Rocks—A

Review of Selected Models and Suggested Work Flows." *Geophysics* 75 (5): 75A31–47.

Bach, Wolfgang, Holger Paulick, Carlos J. Garrido, Benoit Ildefonse, William P. Meurer, and Susan E. Humphris. 2006. "Unraveling the Sequence of Serpentinization Reactions: Petrography, Mineral Chemistry, and Petrophysics of Serpentinites from MAR 15°N (ODP Leg 209, Site 1274)." *Geophysical Research Letters* 33 (13). https://doi.org/10.1029/2006GL025681.

Birch, Francis. 1969. "Density and Composition of the Upper Mantle: First Approximation as an Olivine Layer." *Geophysical Monograph Series* 13:18–36.

Bonnemains, D., J. Carlut, J. Escartin, C. Mevél, M. Andreani, and B. Debret. 2016. "Geochemistry, Geophysics, Geosystems." *Geochemistry Geophysics Geosystems* 17:1312–38. https://doi.org/10.1002/2015GC006205.Received.

Boreham, Christopher J., Dianne S. Edwards, Krystian Czado, Nadege Rollet, Liuqi Wang, Simon van der Wielen, David Champion, Richard Blewett, Andrew Feitz, and Paul A. Henson. 2021. "Hydrogen in Australian Natural Gas: Occurrences, Sources and Resources." *The APPEA Journal* 61 (1): 163. https://doi.org/10.1071/aj20044.

Carlson, R. L. 2001. "The Abundance of Ultramafic Rocks in Atlantic Ocean Crust." *Geophysical Journal International* 144 (1): 37–48. https://doi.org/10.1046/j.0956-540X.2000.01280.x.

Carlson, Richard L, and D Jay Miller. 1997. "- SS Oceanic Gabbro / Diabase." *Most* 24 (4): 457–60.

Castagna, J P, M L Batzle, T K Kan, and M M Backus. 1993. "Rock Physics—The Link between Rock Properties and AVO Response." *Offset-Dependent Reflectivity—Theory and Practice of AVO Analysis: SEG* 8:135–71.

Castagna, John P, Michael L Batzle, and Raymond L Eastwood. 1985. "Relationships between Compressional-Wave and Shear-Wave Velocities in Clastic Silicate Rocks." *Geophysics* 50 (4): 571–81.

Chi, Xin-gang, and De-hua Han. 2009. "Lithology and Fluid Differentiation Using a Rock Physics Template." *The Leading Edge* 28 (1): 60–65.

Christensen, Nikolas I. 1966. "Elasticity of Ultrabasic Rocks." *Journal of Geophysical Research* 71 (24): 5921–31.

———. 1972. "The Abundance of Serpentinites in the Oceanic Crust" 80 (6): 709–19.

———. 1978. "Ophiolites, Seismic Velocities and Oceanic Crustal Structure." *Tectonophysics* 47 (1–2): 131–57. https://doi.org/10.1016/0040-1951(78)90155-5.

———. 2004. "Serpentinites, Peridotites, and Seismology." *International Geology Review* 46 (9): 795–816. https://doi.org/10.2747/0020-6814.46.9.795.

Christensen, Nikolas I., and Matthew H. Salisbury. 1972. "Sea Floor Spreading, Progressive Alteration of Layer 2 Basalts, and Associated Changes in Seismic Velocities." *Earth and Planetary Science Letters* 15 (4): 367–75. https://doi.org/10.1016/0012-821X(72)90037-4.

Coveney Jr., Raymond M, Edwin D Goebel, Edward J Zeller, Gisela A M Dreschhoff, and Ernest E Angino. 1987. "Serpentinization and the Origin of Hydrogen Gas in Kansas1." *AAPG Bulletin* 71 (1): 39–48. https://doi.org/10.1306/94886D3F-1704-11D7-8645000102C1865D.

Cutts, J. A., K. Steinthorsdottir, C. Turvey, G. M. Dipple, R. J. Enkin, and S. M. Peacock. 2021. "Deducing Mineralogy of Serpentinized and Carbonated Ultramafic Rocks Using Physical Properties With Implications for Carbon Sequestration and Subduction Zone Dynamics." *Geochemistry, Geophysics, Geosystems* 22 (9): 1–23. https://doi.org/10.1029/2021GC009989.

Dewandel, Benoît, Françoise Boudier, Hartmut Kern, Waris Warsi, and David Mainprice. 2003. "Seismic Wave Velocity and Anisotropy of Serpentinized Peridotite in the Oman Ophiolite." *Tectonophysics* 370 (1–4): 77–94. https://doi.org/10.1016/S0040-1951(03)00178-1.

Durand, Stéphanie, Marija Putak Juriček, and Karen M. Fischer. 2024. "Hydrous Melting and Its Seismic Signature." *Elements* 20 (4): 241–46. https://doi.org/10.2138/gselements.20.4.241.

Falcon-Suarez, Ismael, Gaye Bayrakci, Tim A. Minshull, Laurence J. North, Angus I. Best, and Stéphane Rouméjon. 2017. "Elastic and Electrical Properties and Permeability of Serpentinites from Atlantis Massif, Mid-Atlantic Ridge." *Geophysical Journal International* 211 (2): 686–99. https://doi.org/10.1093/GJI/GGX341.

Frery, Emanuelle, Laurent Langhi, Mederic Maison, and Isabelle Moretti. 2021. "Natural Hydrogen Seeps Identified in the North Perth Basin, Western Australia." *International Journal of Hydrogen Energy* 46 (61): 31158–73. https://doi.org/10.1016/j.ijhydene.2021.07.023.

Fuad, M I Ahmad, H Zhao, M S Jaya, and E A J Jones. 2023. "SPE-214789-MS Rock Physics Modeling of Hydrogen-Bearing Sandstone : Implications for Natural Hydrogen Exploration and Storage Introduction." https://doi.org/10.2118/214789-MS.

Gardner, G H F, L W Gardner, and ARw Gregory. 1974. "Formation Velocity and Density—The Diagnostic Basics for Stratigraphic Traps." *Geophysics* 39 (6): 770–80.

Gassmann, Fritz. 1951. "Elastic Waves through a Packing of Spheres." *Geophysics* 16 (4): 673–85.

Godfrey, N J, B C Beaudoin, and S L Klemperer. 1997. "Ophiolitic Basement to the Great Valley Forearc Basin, California, from Seismic and Gravity Data: Implications for Crustal Growth at the North American Continental Margin." *Geological Society of America Bulletin* 109 (12): 1536–62.

Hatakeyama, Kohei, and Ikuo Katayama. 2020. "Pore Fluid Effects on Elastic Wave Velocities of Serpentinite and Implications for Estimates of Serpentinization in Oceanic Lithosphere." *Tectonophysics* 775 (November 2019): 228309. https://doi.org/10.1016/j.tecto.2019.228309.

Horen, H., M. Zamora, and G. Dubuisson. 1996. "Seismic Waves Velocities and Anisotropy in Serpentinized Peridotites from Xigaze Ophiolite: Abundance of Serpentine in Slow Spreading Ridge." *Geophysical Research Letters* 23 (1): 9–12. https://doi.org/10.1029/95GL03594.

Huang, Ruifang, Weidong Sun, Maoshuang Song, and Xing Ding. 2019. "Influence of Ph on Molecular Hydrogen (H2) Generation and Reaction Rates during Serpentinization of Peridotite and Olivine." *Minerals* 9 (11). https://doi.org/10.3390/min9110661.

Iturrino, Gerardo J, Nikolas I Christensen, Stephen Kirby, and Matthew H Salisbury. 1991. "11 . SEISMIC VELOCITIES AND ELASTIC PROPERTIES OF OCEANIC GABBROIC ROCKS from Hole 735B" 118:227–44.

Keppler, Hans, Eiji Ohtani, and Xiaozhi Yang. 2024. "The Subduction of Hydrogen: Deep Water Cycling, Induced Seismicity, and Plate Tectonics." *Elements* 20 (4): 229–34. https://doi.org/10.2138/gselements.20.4.229.

Kern, H., and J. M. Tubia. 1993. "Pressure and Temperature Dependence of P- and S-Wave Velocities, Seismic Anisotropy and Density of Sheared Rocks from the Sierra Alpujata Massif (Ronda Peridotites, Southern Spain)." *Earth and Planetary Science Letters* 119 (1–2): 191–205. https://doi.org/10.1016/0012-821X(93)90016-3.

Klein, Frieder, Wolfgang Bach, and Thomas M. McCollom. 2013. "Compositional Controls on Hydrogen Generation during Serpentinization of Ultramafic Rocks." *Lithos* 178:55–69. https://doi.org/10.1016/j.lithos.2013.03.008.

Klein, Frieder, and Véronique Le Roux. 2020. "Quantifying the Volume Increase and Chemical Exchange during Serpentinization." *Geology* 48 (6): 552–56. https://doi.org/10.1130/G47289.1.

Klein, Frieder, Jesse D. Tarnas, and Wolfgang Bach. 2020. "Abiotic Sources of Molecular Hydrogen on Earth." *Elements* 16 (1): 19–24. https://doi.org/10.2138/GSELEMENTS.16.1.19.

Kroenke, L. W., Murli H. Manghnani, C. S. Rai, P. Fryer, and Ralph Ramananantoandro. 2013. "Elastic Properties of Selected Ophiolitic Rocks from Papua New Guinea: Nature and Composition of Oceanic Lower Crust and Upper Mantle" 19 (706): 407–21. https://doi.org/10.1029/gm019p0407.

Lamadrid, Hector M., J. Donald Rimstidt, Esther M. Schwarzenbach, Frieder Klein, Sarah Ulrich, Andrei Dolocan, and Robert J. Bodnar. 2017. "Effect of Water Activity on Rates of Serpentinization of Olivine." *Nature Communications* 8 (July). https://doi.org/10.1038/ncomms16107.

Lefeuvre, N., L. Truche, F. V. Donzé, F. Gal, J. Tremosa, R. A. Fakoury, S. Calassou, and E. C. Gaucher. 2022. "Natural Hydrogen Migration along Thrust Faults in Foothill Basins: The North Pyrenean Frontal Thrust Case Study." *Applied Geochemistry* 145 (October). https://doi.org/10.1016/j.apgeochem.2022.105396.

Lefeuvre, Nicolas, Laurent Truche, Frédéric Victor Donzé, Maxime Ducoux, Guillaume Barré, Rose Adeline Fakoury, Sylvain Calassou, and Eric C. Gaucher. 2021. "Native H2 Exploration in the Western Pyrenean Foothills." *Geochemistry, Geophysics, Geosystems* 22 (8). https://doi.org/10.1029/2021GC009917.

Leong, James Andrew, Michael Nielsen, Noah McQueen, Ruta Karolyte, Darren J. Hillegonds, Chris Ballentine, Tom Darrah, Wade McGillis, and Peter Kelemen. 2023. "H2 and CH4 Outgassing Rates in the Samail Ophiolite, Oman: Implications for Low-Temperature, Continental Serpentinization Rates." *Geochimica et Cosmochimica Acta* 347:1–15. https://doi.org/10.1016/j.gca.2023.02.008.

Li, Zhiyong, Bruce M. Moskowitz, Jianping Zheng, Qing Xiong, Xiang Zhou, Jingsui Yang, Yuwen Zhang, and Qingsheng Liu. 2020a. "Petromagnetic Characteristics of Serpentinization and Magnetite Formation at the Zedang Ophiolite in Southern

Tibet." *Journal of Geophysical Research: Solid Earth* 125 (9). https://doi.org/10.1029/2020JB019696.

———. 2020b. "Petromagnetic Characteristics of Serpentinization and Magnetite Formation at the Zedang Ophiolite in Southern Tibet." *Journal of Geophysical Research: Solid Earth* 125 (9). https://doi.org/10.1029/2020JB019696.

Maffione, Marco, Antony Morris, Oliver Plumper, and Douwe J. J. van Hinsbergen. 2014. "Magnetic Properties of Variably Serpentinized Peridotites and Their Implication for the Evolution of Oceanic Core Complexes." *Geochemistry, Geophysics, Geosystems* 15 (4): 923–44. https://doi.org/10.1002/2013GC004993.

McCollom, Thomas M., Frieder Klein, Mark Robbins, Bruce Moskowitz, Thelma S. Berquó, Niels Jöns, Wolfgang Bach, and Alexis Templeton. 2016. "Temperature Trends for Reaction Rates, Hydrogen Generation, and Partitioning of Iron during Experimental Serpentinization of Olivine." *Geochimica et Cosmochimica Acta* 181:175–200. https://doi.org/10.1016/j.gca.2016.03.002.

McCollom, Thomas M., Frieder Klein, Peter Solheid, and Bruce Moskowitz. 2020. "The Effect of pH on Rates of Reaction and Hydrogen Generation during Serpentinization." *Philosophical Transactions of the Royal Society A: Mathematical, Physical and Engineering Sciences* 378 (2165). https://doi.org/10.1098/rsta.2018.0428.

Mével, Catherine. 2003. "Serpentinisation Des Péridotites Abysales Aux Dorsales Océaniques." *Comptes Rendus - Geoscience* 335 (10–11): 825–52. https://doi.org/10.1016/j.crte.2003.08.006.

Miller, D.J., and N.I. Christensen. 1997. "Seismic Velocities of Lower Crustal and Upper Mantle Rocks from the Slow-Spreading Mid-Atlantic Ridge, South of the Kane Transform Zone (MARK)." *Proceedings of the Ocean Drilling Program, 153 Scientific Results* 153. https://doi.org/10.2973/odp.proc.sr.153.043.1997.

Miller, D.J., G.J. Iturrino, and N.I. Christensen. 1996. "Geochemical and Petrological Constraints on Velocity Behavior of Lower Crustal and Upper Mantle Rocks from the Fast-Spreading Ridge at Hess Deep." *Proceedings of the Ocean Drilling Program, 147 Scientific Results* 147. https://doi.org/10.2973/odp.proc.sr.147.028.1996.

Miller, Hannah M., Lisa E. Mayhew, Eric T. Ellison, Peter Kelemen, Mike Kubo, and Alexis S. Templeton. 2017. "Low Temperature Hydrogen Production during Experimental Hydration of Partially-Serpentinized Dunite." *Geochimica et Cosmochimica Acta* 209:161–83. https://doi.org/10.1016/j.gca.2017.04.022.

Norris, Andrew N. 1985. "A Differential Scheme for the Effective Moduli of Composites." *Mechanics of Materials* 4 (1): 1–16.

Odegaard, E, and Per Avseth. 2004. "Well Log and Seismic Data Analysis Using Rock Physics Templates." *First Break* 22:37–44.

Osselin, F., C. Soulaine, C. Fauguerolles, E. C. Gaucher, B. Scaillet, and M. Pichavant. 2022. "Orange Hydrogen Is the New Green." *Nature Geoscience* 15 (10): 765–69. https://doi.org/10.1038/s41561-022-01043-9.

Oufi, Omar. 2002. "Magnetic Properties of Variably Serpentinized Abyssal Peridotites." *Journal of Geophysical Research* 107 (B5). https://doi.org/10.1029/2001jb000549.

Schön, Jürgen H. 2015. *Physical Properties of Rocks: Fundamentals and Principles of Petrophysics*. Elsevier.

Schouten, Douglas, Donald Furseth, and Jacobus van Nieuwkoop. 2022. "Muon Tomography for Underground Resources." In *Muography: Exploring Earth's Subsurface with Elementary Particles*, 221–35. wiley. https://doi.org/10.1002/9781119722748.ch16.

Stesky, R. M., and W. F. Brace. 1973. "Electrical Conductivity of Serpentinized Rocks to 6 Kilobars." *Journal of Geophysical Research* 78 (32): 7614–21. https://doi.org/10.1029/jb078i032p07614.

Templeton, Alexis S., Eric T. Ellison, Peter B. Kelemen, James Leong, Eric S. Boyd, Daniel R. Colman, and Juerg M. Matter. 2024. "Low-Temperature Hydrogen Production and Consumption in Partially-Hydrated Peridotites in Oman: Implications for Stimulated Geological Hydrogen Production." *Frontiers in Geochemistry* 2:1–20. https://doi.org/10.3389/fgeoc.2024.1366268.

Toft, Paul B, Jafar Arkani-Hamed, and Stephen E Haggerty. 1990. "The Effects of Serpentinization on Density and Magnetic Susceptibility: A Petrophysical Model." *Physics of the Earth and Planetary Interiors* 65:137–57.

Truche, Laurent, Thomas M. McCollom, and Isabelle Martinez. 2020. "Hydrogen and Abiotic Hydrocarbons: Molecules That Change the World." *Elements* 16 (1): 13–18. https://doi.org/10.2138/GSELEMENTS.16.1.13.

Watanabe, Tohru, Hiroaki Kasami, and Shohei Ohshima. 2007. "Compressional and Shear Wave Velocities of Serpentinized Peridotites up to 200 MPa." *Earth, Planets and Space* 59 (4): 233–44. https://doi.org/10.1186/BF03353100.

Yoshino, Takashi, Geeth Manthilake, and Anne Pommier. 2024. "Probing Deep Hydrogen Using Electrical Conductivity." *Elements* 20 (4): 247–52. https://doi.org/10.2138/gselements.20.4.247.

Zimmerman, Robert Wayne. 1990. "Compressibility of Sandstones."